Journal of Applied Spectroscopy, Vol. 79, No. 5, November, 2012 (Russian Original Vol. 79, No. 5, September–October, 2012)

RAMAN SPECTRA OF TETRAOXA[8]CIRCULENES. *p*-DINAPHTHALENODIPHENYLENOTETRAFURAN AND ITS TETRAALKYL DERIVATIVES (DFT STUDY AND EXPERIMENT)

V. A. Minaeva,[a*] B. F. Minaev,[a] G. V. Baryshnikov,[a] O. N. Romeyko,[a] and M. Pittelkow[b]

UDC 544.174.2

The equilibrium molecular geometry, harmonic vibrational frequencies, and Raman band intensities were calculated by the density functional theory B3LYP method with the 6-31G(d) basis set for tetraoxa[8]circulenes p-dinaphthalenodiphenylenotetrafuran (p-2B2N) and p-dinaphthaleno-2,3,10,11-tetraethyldiphenylenotetrafuran (p-2B2N4R, R = C_2H_5) whose molecules belong to D_{2h} and D_2 point group symmetry. All bands in the measured Raman spectrum of p-dinaphthaleno-2,3,10,11-tetraundecyldiphenylenotetrafuran (p-2B2N4R, R = n-$C_{11}H_{23}$) were assigned based on quantum-chemical calculations of the frequencies and normal vibration modes of the molecule. A comparison of the calculated vibrational spectra with those from the experiment made it possible to assign reliably all observed bands in the Raman spectrum. Results of quantum-chemical calculations were in good agreement with the experimental data.

Keywords: *tetraoxa[8]circulene, DFT/B3LYP/6-31G(d) calculations, density functional theory, Raman spectrum, point group symmetry, benzene, naphthalene, furan.*

Introduction. Tetraoxa[8]circulenes and their heteroatomic analogs (octathia[8]circulene, tetrathiatetraselena[8]circulene, etc.) are condensed planar heterocyclic compounds [1–3] that hold promise in microelectronics and nanophotonics [4–7]. In particular, tetraoxa[8]circulenes luminesce intensely upon excitation by an electric field. This made it possible to use them as organic light-emitting diodes in electroluminescent layers [4, 5]. Tetraoxa[8]circulenes are also of great theoretical interest as highly symmetric macroheterocyclic molecules. Their structures and spectral properties have recently been studied extensively. The structure and electronic absorption spectra of the simplest symmetric tetraoxa[8]circulene **1a** were studied theoretically by Minaev et al. [8]. Vibrational spectra of several symmetric tetraoxa[8]circulenes (in particular, **1a** and **1c**) were studied in detail [9, 10]. Herein we present new data on line assignments in the Raman spectrum recorded by us of the tetraoxa[8]circulene *p*-dinaphthaleno-2,3,10,11-tetraundecyldiphenylenotetrafuran (**1b**) (*p*-2B2N4R, R = *n*-$C_{11}H_{23}$).

Experimental. Tetraoxa[8]circulene *p*-2B2N4R (R = *n*-$C_{11}H_{23}$) was synthesized by statistical condensation of 2,3-*bis*-undecyl-1,4-benzoquinone and naphthoquinone according to the original method [4]. The various isomers were separated and purified over a chromatography column packed with silica gel. Raman spectra were recorded on a Bruker IFS66 NIR-FT spectrometer equipped with an FRA106 module. The excitation source was a Nd:YAG laser emitting at λ = 1064 nm with output power 300 mW. A Ge diode cooled to liquid-nitrogen temperature was used as the detector.

Calculations. The *n*-undecyl substituents in *p*-2B2N4R (R = $C_{11}H_{23}$) were replaced by ethyl groups (*p*-2B2N4R, R = C_2H_5) or H atoms (*p*-2B2N4R, R = H, further designated *p*-2B2N, Fig. 1) in order to simplify the calculations.

*To whom correspondence should be addressed.

[a]Bohdan Khmelnytsky National University of Cherkassy, 81 Schevchenko Bulv., Cherkassy, 18031, Ukraine; e-mail: bfmin@rambler.ru; [b]Copenhagen University, Denmark, DK-2100; e-mail: pittel@kiku.dk. Translated from Zhurnal Prikladnoi Spektroskopii, Vol. 79, No. 4, pp. 709–720, September–October, 2012. Original article submitted May 5, 2012.

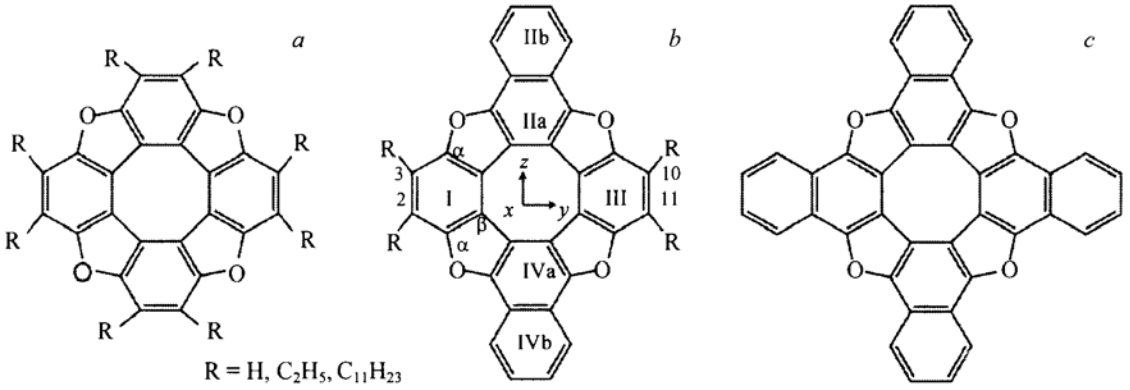

Fig. 1. Structures of π-conjugated tetraoxa[8]circulenes 4B (a), *p*-2B2N (b), and 4N (c).

The structures of *p*-2B2N and *p*-2B2N4R (R = C_2H_5) were optimized using density functional theory B3LYP/6-31G(d) [11, 12] in the Gaussian 03 program package [11] with monitoring of the maximally possible symmetry. Frequencies and the corresponding activities of normal modes (NM) were also calculated using this method. All frequencies of vibrations were real, indicating that a true minimum on the hypersurface of the total molecular energy was found. The calculated frequencies were adjusted for comparison with the experimental values. Various scaling factors were used for different spectral ranges, i.e., 0.950 for the high-frequency range and 0.969 for other spectral ranges. The scaling factors were obtained as the average of ratios of experimental and calculated NM frequencies of all fragments in a certain spectral range. The scaling factors were typical of corresponding spectral ranges [12].

The NM activities in Raman spectra (S_i) that were calculated by density functional theory were not identical to the observed Raman intensities because calculation of Raman activities did not account for excitation energy of the molecules by the laser radiation. We used the recalculation formula that was used before [13, 14] to transform the Raman activity into the corresponding intensity for the *i*-th NM (I_i):

$$I_i = \frac{f(\nu_0 - \nu_i)^4 S_i}{\nu_i [1 - \exp(-hc_0\nu_i/kT)]},$$

where ν_0 is the exciting laser frequency (9398.5 cm^{-1}); ν_i, the frequency of the i-th NM (cm^{-1}); c_0, the speed of light in a vacuum ($2.9979 \cdot 10^{10}$ cm/s); *h*, Planck's constant ($6.6261 \cdot 10^{-27}$ erg·s); *k*, Boltzmann's constant ($1.3806 \cdot 10^{-16}$ erg/K); and *f*, an arbitrarily selected recalculation factor for all peaks (taken as equal to unity).

Calculated I_i values were normalized to unity for comparison with the corresponding normalized experimental spectra. A comparison of the calculated vibrational spectra of *p*-2B2N4R (R = C_2H_5) and *p*-2B2N with the measured Raman spectrum of *p*-2B2N4R (R = $C_{11}H_{23}$) enabled Raman lines corresponding to vibrations of the alkyl substituents to be found in the experimental spectrum. The calculated spectra of the studied tetraoxa[8]circulenes were constructed using the SWizard program [15] (line half-width 15 cm^{-1}, Lorentz distribution function). The form of the NM was determined by varying the calculated form of the NM.

Results and Discussion. ***Molecular geometry of p-dinaphthalenodiphenylenotetrafuran.*** Replacing two benzene rings in tetraphenylenotetrafuran (4B) by naphthalene fragments (Fig. 1) formed *p*-2B2N, which belonged to point group symmetry D_{2h}. The geometric parameters of the naphthalene fragments (rings IIa, IIb and IVa, IVb) were similar to the corresponding parameters of tetranaphthalenotetrafuran (4N) whereas those of the benzene rings (rings I and III) in *p*-2B2N were similar to those in 4B. The furan rings became asymmetric. The C–C bonds in the cyclooctatetraene (CT) ring were not strictly alternating, in contrast with 4B [9]. The outer π-conjugated perimeter increased in the series of molecules 4B, *p*-2B2N, and 4N.

Addition of ethyl substituents increased the $C^{2(3)}$–C^{α}, C^{α}–O, and C^2–C^3 bond lengths by 0.008, 0.005, and 0.014 Å, respectively, compared with unsubstituted *p*-2B2N. Thus, the C^{α}–C^{β} bond length decreased by 0.004 Å. This

was due to the manifestation of a weak positive inductive effect of the ethyl substituents. This agreed with published x-ray structure data [6].

Raman spectra of p-2B2N and p-2B2N4R (R = C_2H_5 and $C_{11}H_{23}$). The vibrational spectrum of tetraoxa [8]circulene *p*-2B2N, which consists of 48 atoms, contains 138 NM that are distributed in point group D_{2h} among symmetry types as follows:

$$\Gamma_{tot} + 12A_u + 11B_{1g}\,(R) + 11B_{3u}\,(IR) + 11B_{2g}\,(R) + 23B_{2u}\,(IR) + 23B_{1u}\,(IR) + 23B_{3g}\,(R) + 24A_g\,(R)\,.$$

In-plane vibrations of symmetry B_{1u} and B_{2u} and out-of-plane vibrations B_{3u} are active in the IR spectrum. In-plane vibrations A_g, B_{3g} and out-of-plane B_{1g}, B_{2g} can appear in the Raman spectrum. Out-of-plane vibrations of symmetry A_u are inactive in IR and Raman spectra.

The vibrational spectrum of *p*-2B2N4R (R = C_2H_5), which consists of 78 atoms, contains 210 NM that are distributed in point group D_2 (macrocycle in the *xy* plane) among symmetry types as follows: 54*A*, 52B_1, 52B_2, and 52B_3. Vibrations of symmetry B_1, B_2, and B_3 are active in the IR spectrum. There are no symmetry restrictions for the Raman spectrum although vibrations of symmetry *A* are more active.

Tables 1 and 2* present forms of vibrations, calculated frequencies, and NM activities of *p*-2B2N and *p*-2B2N4R (R = C_2H_5) and give line assignments in the experimental Raman spectrum of *p*-2B2N4R (R = $C_{11}H_{23}$). Figures 2 and 3 show calculated Raman spectra for *p*-2B2N4R (R = H, C_2H_5), 4B, 4N, benzene, furan, and naphthalene for spectral ranges 3300–2800 and 1700–0 cm^{-1} and compare them with the experimental spectrum of *p*-2B2N4R (R = $C_{11}H_{23}$).

CH vibrations of aromatic rings. CH vibrations in Raman spectra of aromatic compounds can be identified in the ranges 3080–3010 cm^{-1} [ν(CH)] and 1290–990 cm^{-1} (in-plane CH bending) and below 900 cm^{-1} (out-of-plane CH bending) [16]. Six vibrational modes of symmetry A_g and B_{3g} belong to C–H stretching vibrations in the Raman spectrum of unsubstituted circulene *p*-2B2N. Benzene ν(CH) vibrations ν_{138} and ν_{135} were calculated by us with greater frequencies compared with naphthalene ν_{134}, ν_{131}, ν_{130}, and ν_{127} (Table 1). Fully symmetric vibrations were more active and had greater frequencies compared with those of lower symmetry. Weak lines at 3072 [$\nu(CH)_{benz}$], 3059, 3043, and 3031 cm^{-1} [$\nu(CH)_{naph}$] belonged to C–H stretching vibrations in the calculated Raman spectrum of *p*-2B2N (Fig. 3). A slight shift toward greater frequencies compared with ν(CH) in benzene and naphthalene was observed upon forming *p*-2B2N. This was a consequence of the measurement of the geometric parameters upon condensation of the benzene and naphthalene rings. The ν(CH) frequencies were not shifted when compared with analogous vibrations in Raman spectra of 4B and 4N [9] (Fig. 2).

The ν(CH) vibrations of naphthalene fragments in the calculated Raman spectrum of substituted circulene *p*-2B2N4R (R = C_2H_5) had the same frequencies as for unsubstituted circulene *p*-2B2N. However, the corresponding line in the experimental spectrum of *p*-2B2N4R (R = $C_{11}H_{23}$) was weak. In-plane bending vibrations δ(CH) in the Raman spectrum of *p*-2B2N were calculated by us in the range 1276–985 cm^{-1} (Table 1, Fig. 3). As a rule, these vibrations were mixed with ν(CO) of furan rings and/or with in-plane ring bendings.

Replacement of two benzene fragments in 4B by naphthalene fragments led to mixing of their δ(CH) vibrations (Fig. 4a).

The NM ν_{90}, ν_{88}, and ν_{85} in the spectrum of *p*-2B2N contained δ(CH) vibrations of only naphthalene fragments. Of these, ν_{88} (ν_{calc} = 1159 cm^{-1}) belonged exclusively to δ(CH) vibrations. Benzene and naphthalene δ(CH) vibrations and also other types of vibrations contributed to NM ν_{96}, ν_{94}, ν_{91}, ν_{83}, ν_{82}, and ν_{77}. It should be noted that forbidden NM ν_{67} in the Raman spectrum of 4B and ν_{116} in that of 4N of symmetry A_{2g} in the Raman spectrum of *p*-2B2N gave weakly active vibration ν_{91} of symmetry B_{3g} with frequency 1208 cm^{-1}. However, it was not seen in the spectrum in Fig. 3 because it was overlapped by the stronger line at 1207 cm^{-1} (ν_{90}). The last line contributed not only to δ(CH) vibrations of the naphthalene fragments but also to vibrations of fragments for which the geometry was affected by introducing the alkyl substituents (Table 2). This led to a shift of the corresponding line in the spectrum of *p*-2B2N4R (R = C_2H_5) to 1233 cm^{-1}. In our opinion, the long shoulder on the low-frequency side of the line at 1241 cm^{-1} corresponded to this line in the experimental spectrum of *p*-2B2N4R (R = $C_{11}H_{23}$).

*Complete tables are available by e-mail from the authors.

TABLE 1. Calculated Data for Raman-Active Normal Modes of *p*-2B2N

Mode	Symmetry	ν, cm^{-1}	S_i, $Å^4$ /a.m.u.	I_i	Vibration type
ν_{138}	A_g	3072	610.4	$3.3\cdot10^{-2}$	ν_s(CH) I, III in ph.
ν_{135}	B_{3g}	3060	133.7	$7.4\cdot10^{-3}$	ν_{as}(CH) I, III
ν_{134}	A_g	3059	839.1	$4.6\cdot10^{-2}$	ν_s(CH) II, IV in ph.
ν_{131}	B_{3g}	3054	207.3	$1.1\cdot10^{-2}$	ν_{as}(CH) II, IV
ν_{130}	A_g	3043	449.1	$2.5\cdot10^{-2}$	ν_{as}(CH) II, IV
ν_{127}	B_{3g}	3031	136.4	$7.7\cdot10^{-3}$	ν_{as}(CH) II, IV
ν_{126}	A_g	1637	2750.4	0.7	ν_s(CH) I–IV in ph.; $\nu(C^{\beta}C^{\beta'})$ in ph.
ν_{124}	B_{3g}	1628	815.4	0.2	ν_s(CC) II, IV oo ph.; $\nu_{as}(C^{\alpha}C^{\beta})$
ν_{121}	B_{3g}	1600	654.7	0.2	ν_s(CC) I, III oo ph.; $\nu_{as}(C^{\alpha}C^{\beta})$
ν_{119}	A_g	1585	95.3	$2.6\cdot10^{-2}$	ν_s(CC) I, III and II, IV oo ph.
ν_{118}	B_{3g}	1583	446.9	0.1	ν_s(CC) IIa, IVa; ν_{as}(CH) IIb, IVb; $\delta(\angle COC)$
ν_{115}	A_g	1540	278.5	$7.9\cdot10^{-2}$	ν_{as}(CC) II, IV; $\nu(C^{\beta}C^{\beta'})$; $\delta(\angle COC)$
ν_{114}	A_g	1475	2045.4	0.6	ν_{as}(CC) I–IV; $\nu(C^{\beta}C^{\beta'})$; $\nu_s(C^{\alpha}C^{\beta})$
ν_{111}	B_{3g}	1452	20.9	$6.6\cdot10^{-3}$	In-plane as def. IIa, IVa; ν_{as}(CC) I, III
ν_{110}	A_g	1431	63.0	$2.1\cdot10^{-2}$	ν_{as}(CC) I, III and II, IV oo ph.
ν_{107}	A_g	1422	3043.9	1.0	ν_{as}(CC) Kekule I, III, IIa, IVa; $\delta(\angle COC)$
ν_{106}	B_{3g}	1418	317.8	0.1	ν_{as}(CC) I, III; $\nu(C^{\beta}C^{\beta'})$
ν_{103}	B_{3g}	1381	13.6	$4.7\cdot10^{-3}$	ν_s(CO); $\delta(\angle COC)$; $\nu(C^{\beta}C^{\beta'})$
ν_{102}	A_g	1358	92.0	$3.3\cdot10^{-2}$	ν_{as}(CC) Kekule I, III, IIa, IVa
ν_{99}	B_{3g}	1336	125.6	$4.6\cdot10^{-2}$	In-plane as def. IIa, IVa; ν_s(CO); $\nu(C^{\beta}C^{\beta'})$
ν_{98}	A_g	1331	92.5	$3.4\cdot10^{-2}$	ν_{as}(CC) Kekule IIb, IVb in ph.
ν_{96}	A_g	1276	1492.3	0.6	ν_s(CO); def. I, III, IIa, IVa in ph., CT oo ph. ν_{as}(CC) Kekule IIb, IVb; ν_{as}(CC) I, III, δ(CH) I –IV
ν_{94}	B_{3g}	1249	11.7	$4.8\cdot10^{-3}$	δ(CH) II, IV oo ph.; δ(CH) I, III oo ph.
ν_{91}	B_{3g}	1208	19.0	$8.2\cdot10^{-3}$	δ(CH) I, III; ν(CO) "breathing" of rings
ν_{90}	A_g	1207	249.9	0.1	δ(CH) II, VI; ν_{as}(CO); def. I, III and CT IIa, IVa oo ph.
ν_{88}	A_g	1159	41.0	$1.9\cdot10^{-2}$	δ(CH) II, VI in ph.
ν_{83}	A_g	1119	68.5	$3.4\cdot10^{-2}$	δ(CH) I, III; def. CT, fur., ν(CO)
ν_{82}	A_g	1071	35.1	$1.8\cdot10^{-2}$	δ(CH) I–IV; ν(CO) "breathing" of rings; def. CT, IIa, IVa
ν_{77}	A_g	1025	1.9	$1.1\cdot10^{-3}$	δ(CH) II, IV in ph.; def. I–IV, CT
ν_{73}	A_g	985	780.5	0.5	"Breathing" of rings IIb, IVb and CT oo ph.; δ(CH) I, III in ph; sym, def. I, III, fur
ν_{64}	B_{1g}	855	6.8	$5.0\cdot10^{-3}$	γ_{as}(CH) II, IV in ph.
ν_{45}	B_{2g}	659	13.0	$1.4\cdot10^{-2}$	γ(CH) II, IV oo ph.; out-of-plane def IIa, IVa oo ph.
ν_{35}	A_g	543	0.4	$6.2\cdot10^{-4}$	"Breathing" I, III, fur., CT in ph. and II, IV oo ph.
ν_{21}	A_g	372	26.9	$6.7\cdot10^{-2}$	"Breathing" I–IV, fur., CT in ph.
ν_{12}	A_g	233	42.7	0.2	"Breathing" I, III, CT and II, IV oo ph.
ν_{11}	B_{2g}	229	10.2	$5.8\cdot10^{-2}$	Out-of-plane def. I –IV, fur., CT
ν_{10}	B_{1g}	197	12.7	$8.7\cdot10^{-2}$	Out-of-plane def. I –IV, CT
ν_9	B_{3g}	174	1.6	$1.4\cdot10^{-2}$	In-plane skeleton rocking
ν_5	B_{1g}	123	3.8	$6.0\cdot10^{-2}$	Out-of-plane rocking of ring IIb, IVb in ph.
ν_3	B_{2g}	77	6.3	0.2	Out-of-plane rocking of ring IIb, IVb oo ph.

Note. S_i, Raman activity; I_i, relative intensity of Raman lines; I, III, numbering of benzene rings; II(a, b), IV(a, b), numbering of naphthalene rings; CT, cyclooctatetraene ring; fur, furan ring; def, bending; as, asymmetric; sym, symmetric; oo ph, out of phase; ν, stretching; δ, planar bending; γ, out-of-plane bending.

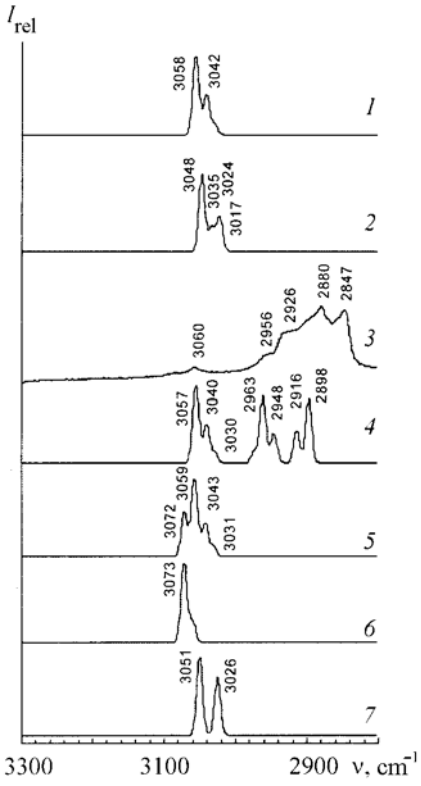

Fig. 2. Theoretical (1, 2, 4–7) and experimental (3) Raman spectra of benzene (7), naphthalene (2), and compounds 4B (6), 4N (1), and *p*-2B2N4R [R = H (5), C_2H_5 (4), $C_{11}H_{23}$ (3)] in the high-frequency range.

The NM ν_{73} (ν_{calc} = 985 cm^{-1}) contributed to δ(CH) vibrations of only benzene fragments in addition to ν(CO) of furan rings and breathing of CT and naphthalene rings. The δ(CH) vibrations were missing in the corresponding vibration (ν_{97}) in the Raman spectrum of substituted *p*-2B2N4R (R = C_2H_5). This caused a low-frequency shift by 25 cm^{-1} of the line in the Raman spectrum and decreased its intensity. Another large shift of the corresponding line (ν_{exp} = 936 cm^{-1}, Fig. 3) was observed in the experimental spectrum of *p*-2B2N4R (R = $C_{11}H_{23}$). The δ(CH) line in the naphthalene fragments that was calculated by us in the spectrum of 4N at 1157 cm^{-1}; of *p*-2B2N, at 1159 cm^{-1}, was observed at these same frequencies in Raman spectra of substituted *p*-2B2N4R molecules and with similar intensities (Fig. 3) because the geometric parameters of the naphthalene fragments of 4N were similar to the corresponding parameters of *p*-2B2N4R and *p*-2B2N4R (R = C_2H_5).

Out-of-plane CH bending vibrations of benzene and naphthalene rings γ(CH) of symmetry B_{1g} and B_{2g} in the Raman spectrum of *p*-2B2N were calculated in the range 960–634 cm^{-1}. The γ(CH) bendings were mixed with out-of-plane bendings of benzene and naphthalene rings at 756 cm^{-1} and lower. The corresponding lines were not found in Raman spectra of *p*-2B2N and *p*-2B2N4R in Fig. 3 because of their low intensity with the exception of very weak lines for γ(CH) of naphthalene rings at 855 cm^{-1} [854 cm^{-1} for *p*-2B2N4R (R = C_2H_5), ν_{exp} = 857 cm^{-1}] and 659 cm^{-1} [650 cm^{-1} for *p*-2B2N4R (R = C_2H_5)].

CH vibrations of methyl and methylene groups of alkyl substituents. Calculated frequencies 2963, 2948, 2916, and 2898 cm^{-1} (Fig. 2) belonged to vibrations of C–H bonds in CH_2- and CH_3-groups of the substituents. These lines in the experimental Raman spectrum of *p*-2B2N4R (R = $C_{11}H_{23}$) were shifted to lower frequencies and were observed as a broad band with maxima at 2880 and 2847 cm^{-1} and a broad shoulder on the high-frequency side. In our opinion, such a shift was related to the increased length of the C–H chain and with intermolecular interactions of the long

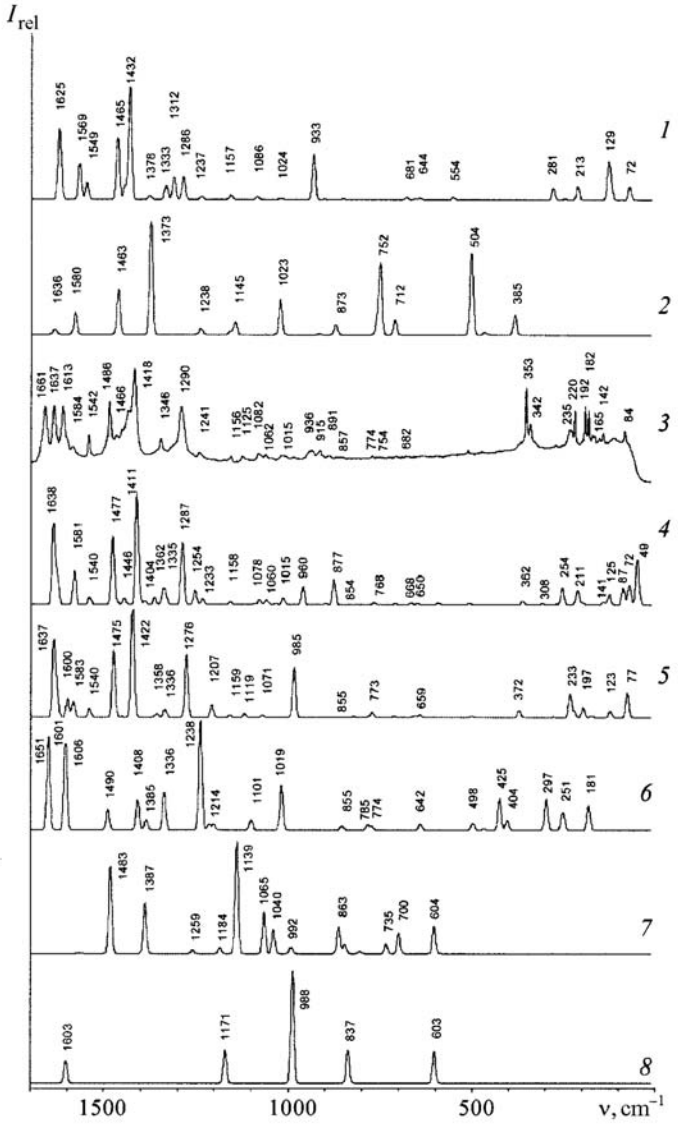

Fig. 3. Calculated (1, 2, 4-8) and experimental (3) Raman spectra of symmetric compounds 4N (1), naphthalene (2), *p*-2B2N4R [R = $C_{11}H_{23}$ (3), C_2H_5 (4), H (5)], 4B (6), furan (7), and benzene (8).

aliphatic substituents in the crystalline state of the circulene. In the Raman spectrum of undecane [17], CH stretching vibrations had frequencies 2963, 2936, 2892, 2876, and 2864 cm^{-1}.

Asymmetric bending vibrations of methyl [$\delta_{as}(CH_3)$] in substituted *p*-2B2N4R (R = C_2H_5) corresponded to NM ν_{164}–ν_{161} with frequency 1480 cm^{-1} and ν_{170}–ν_{165} in the range 1499–1484 cm^{-1} that were mixed with scissors vibrations of methylenes [$b(CH_2)$]. The line corresponding to them in spectra of *p*-2B2N4R was overlapped by a strong line at 1477 cm^{-1} (ν_{exp} = 1486 cm^{-1}) that belonged to CC stretching vibrations in benzene, naphthalene, and furan rings. Scissors vibrations of methylene groups that were not mixed with other types of vibrations had calculated frequency 1465 cm^{-1} (ν_{exp} = 1466 cm^{-1}).

Symmetric bending vibrations of methyls [$\delta_s(CH_3)$] were calculated in the narrow frequency range 1392–1390 cm^{-1} and did not form an independent line in spectra of *p*-2B2N4R. Twisting vibrations of methyls [$\tau(CH_3)$] were calculated by us in the range 1093–1051 cm^{-1} and in the low-frequency range 290–169 cm^{-1}; rocking vibrations [$r(CH_3)$], below 820 cm^{-1}. Figure 3 shows the spectrum of *p*-2B2N4R (R = C_2H_5). The contribution of $\tau(CH_3)$ vibra-

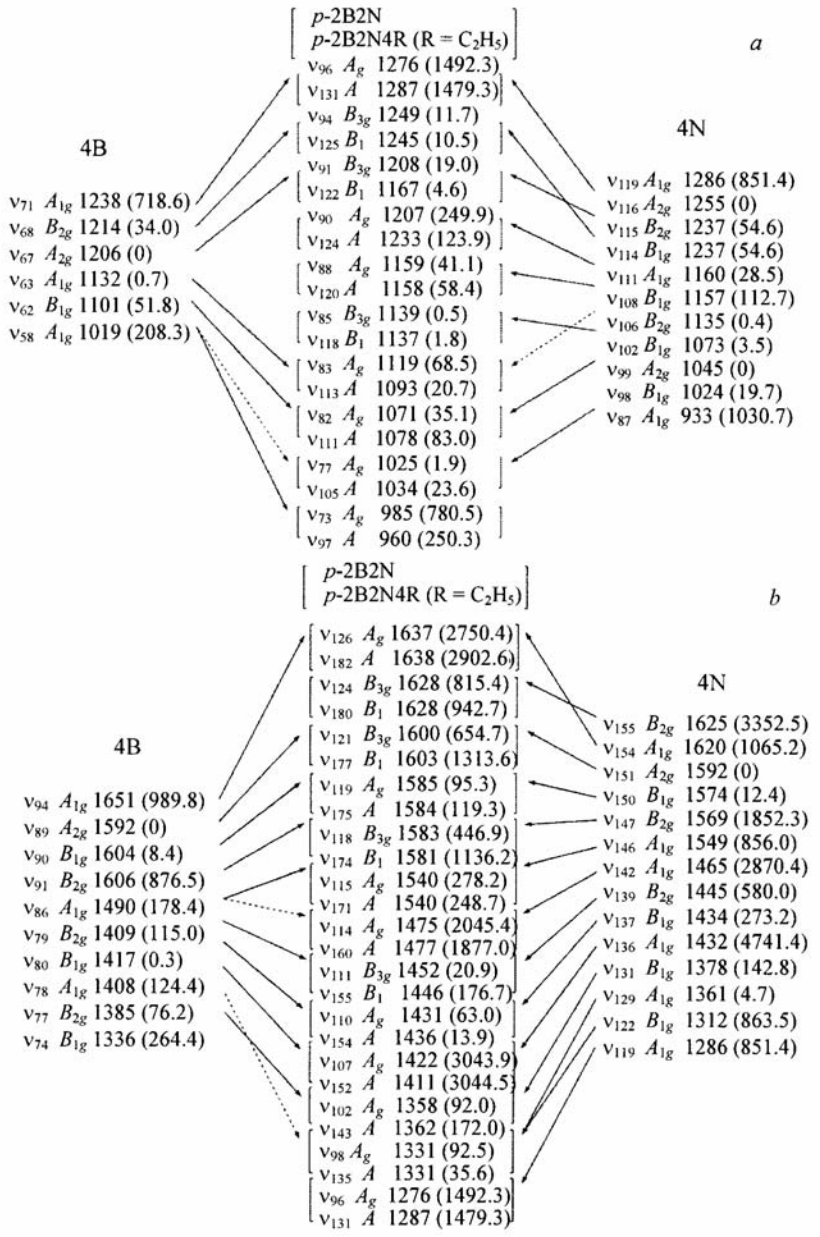

Fig. 4. Combination of Raman-active δ(CH) (a) and ν(CC) (b) vibrational modes of benzene and naphthalene fragments to form the corresponding Raman-active normal vibrations of *p*-2B2N4R (R = H and C_2H_5); numbers in parentheses after frequencies correspond to the calculated activity S_i of the *i*-th normal modes in the Raman spectrum, $Å^4$/a.m.u.; dashed lines denote weak contributions of aromatic ring ν(CC) vibrations.

tions gave weak lines at 1060 cm^{-1} (ν_{exp} = 1062 cm^{-1}) and 211 cm^{-1} (ν_{exp} = 220 cm^{-1}). The contribution of $r(CH_3)$ had lines at 768, 254, and 141 cm^{-1} (ν_{exp} = 774, 235, and 142 cm^{-1}, respectively).

Wagging [$\omega(CH_2)$] and twisting vibrations of methylene groups [$\tau(CH_2)$] were calculated in the range 1332–1034 cm^{-1} (Table 2). A weak line at 1254 cm^{-1} (ν_{exp} = 1241 cm^{-1}) belonged exclusively to methylene twisting vibrations $\tau(CH_2)$ that were mixed with $\tau(CH_3)$ and formed a weak line at 1060 cm^{-1} (ν_{exp} = 1062 cm^{-1}). Wagging vibrations were less active in the Raman spectrum.

TABLE 2. Calculated Data for Raman-Active Normal Modes of *p*-2B2N4R (R = C_2H_5)

Mode	Symmetry	ν, cm^{-1}	S_i, $Å^4$ /a.m.u.	I_i	R=$C_{11}H_{23}$ (exp.)	Vibration type
ν_{210}	A	3057	834.3	$4.5\cdot10^{-2}$	3060	ν_s(CH) II, IV in ph.
ν_{207}	B_1	3052	189.7	$1.0\cdot10^{-2}$		ν_{as}(CH) II, IV oo ph.
ν_{206}	A	3040	450.7	$2.5\cdot10^{-2}$		ν_{as}(CH) II, IV in ph.
ν_{203}	B_1	3030	128.9	$7.2\cdot10^{-3}$		ν_{as}(CH) II, IV oo ph.
ν_{202}	A	2975	78.7	$4.7\cdot10^{-3}$		$\nu_{as}(CH_3, CH_2)$
ν_{198}	A	2963	347.4	$2.1\cdot10^{-2}$		$\nu_{as}(CH_3, CH_2)$
ν_{195}	B_1	2962	381.6	$2.3\cdot10^{-2}$		$\nu_{as}(CH_3, CH_2)$
ν_{194}	A	2948	157.9	$9.6\cdot10^{-3}$		$\nu_{as}(CH_3, CH_2)$
ν_{193}	B_3	2948	105.9	$6.4\cdot10^{-3}$		$\nu_{as}(CH_3, CH_2)$
ν_{192}	B_2	2943	64.8	$4.0\cdot10^{-3}$		$\nu_{as}(CH_3, CH_2)$
ν_{190}	A	2916	259.7	$1.6\cdot10^{-2}$	2880	$\nu_s(CH_2)$ in ph.
ν_{186}	A	2898	602.4	$3.9\cdot10^{-2}$	2847	$\nu_s(CH_3)$ in ph.
ν_{185}	B_1	2898	53.2	$3.4\cdot10^{-3}$		$\nu_s(CH_3)$ I, III oo ph.
ν_{182}	A	1638	2902.6	0.7	1661	ν_s(CC) I–IV in ph.; $\nu(C^{\beta}C^{\beta'})$ in ph.
ν_{180}	B_1	1628	942.7	0.2	1637	ν_s(CC) II, IV oo ph.; $\nu_{as}(C^{\alpha}C^{\beta})$
ν_{177}	B_1	1603	1313.6	0.3	1613	ν_s(CC) I, III oo ph.; $\nu_{as}(C^{\alpha}C^{\beta})$
ν_{175}	A	1584	119.3	$3.2\cdot10^{-2}$	1584	ν_s(CC) I, III and II, IV oo ph.
ν_{174}	B_1	1581	1136.2	0.3	1584	ν_s(CC) IIa, IVa; ν_{as}(CC) IIb, IVb; $\delta(\angle COC)$
ν_{171}	A	1540	248.7	$7.0\cdot10^{-2}$	1542	ν_{as}(CC) II, IV; ν_{as}(CC) I, III; $\nu(C^{\beta}C^{\beta'})$; $\delta(\angle COC)$
ν_{170}	A	1499	22.0	$6.5\cdot10^{-3}$		$b(CH_2)$ in ph.; $\delta_{as}(CH_3)$
ν_{167}	B_2	1489	4.1	$1.2\cdot10^{-3}$		$b(CH_2)$ in ph.; $\delta_{as}(CH_3)$
ν_{166}	A	1484	35.0	$1.1\cdot10^{-2}$		$\delta_{as}(CH_3)$; $b(CH_2)$ in ph.
ν_{165}	B_3	1484	28.0	$8.4\cdot10^{-3}$		$\delta_{as}(CH_3)$; $b(CH_2)$ II, IV oo ph.
ν_{164}	B_1	1480	19.9	$6.0\cdot10^{-3}$		$\delta_{as}(CH_3)$
ν_{163}	B_2	1480	9.3	$2.8\cdot10^{-3}$		$\delta_{as}(CH_3)$
ν_{162}	A	1480	148.5	$4.5\cdot10^{-2}$		$\delta_{as}(CH_3)$
ν_{160}	A	1477	1877	0.6	1486	ν_{as}(CC) I–IV in ph; $\nu(C^{\beta}C^{\beta'})$; $\nu_s(C^{\alpha}C^{\beta})$
ν_{159}	B_2	1465	69.1	$2.1\cdot10^{-2}$	1466	$b(CH_2)$ I, III in ph.
ν_{158}	B_1	1465	11.7	$3.6\cdot10^{-3}$		$b(CH_2)$ I, III oo ph.
ν_{155}	B_1	1446	176.7	$5.6\cdot10^{-2}$		In-plane as def of rings IIa, IVa; ν_{as}(CC) I, III
ν_{154}	A	1436	13.9	$4.4\cdot10^{-3}$		ν_{as}(CC) I, III and II, IV oo ph.
ν_{152}		1411	3044.5	1.0	1418	ν_{as}(CC) Kekule I, III, IIa, IVa; $\delta(\angle COC)$
ν_{150}	B_1	1404	220.0	$7.3\cdot10^{-2}$		ν_{as}(CC) I, III; $\nu(C^{\beta}C^{\beta'})$
ν_{146}	A	1390	102.0	$3.4\cdot10^{-2}$		$\delta_s(CH_3)$ I, III in ph.
ν_{143}	A	1362	172.0	$6.0\cdot10^{-2}$		ν_{as}(CC) Kekule I, III, IIa, IVa
ν_{142}	B_1	1361	10.6	$3.7\cdot10^{-3}$		ν_s(CO); $\nu(C^{\beta}C^{\beta'})$; $\delta(\angle COC)$
ν_{139}	A	1341	214.1	$7.7\cdot10^{-2}$	1346	ν_{as}(CC) Kekule IIb, IVb; ν_s(CO); def. I, III, CT
ν_{138}	B_1	1335	244.5	$8.8\cdot10^{-2}$	1346	In-plane as def of rings IIa, IVa; ν_s(CO); $\nu(C^{\beta}C^{\beta'})$
ν_{136}	B_2	1332	9.8	$3.6\cdot10^{-3}$		$\omega(CH_2)$
ν_{135}	A	1331	35.6	$1.3\cdot10^{-2}$		ν_{as}(CC) Kekule IIb, IVb in ph.
ν_{134}	B_1	1328	55.7	$2.0\cdot10^{-2}$		$\omega(CH_2)$ oo ph.
ν_{131}	A	1287	1479.3	0.6	1290	ν_s(CO); def. I, III, IIa, IVa in ph., CT oo ph. ν_{as}(CC) Kekule IIb, IVb; δ(CH) II, IV
ν_{130}	B_1	1267	6.0	$2.4\cdot10^{-3}$		$\tau(CH_2)$

TABLE 2. (Continued)

Mode	Symmetry	ν, cm^{-1}	S_i, $Å^4$ /a.m.u.	I_i	R=$C_{11}H_{23}$ (exp.)	Vibration type
ν_{128}	B_2	1266	5.1	$2.0\cdot10^{-3}$		$\tau(CH_2)$
ν_{127}	A	1254	312.2	0.1	1241	$\tau(CH_2)$
ν_{126}	B_3	1253	6.5	$2.6\cdot10^{-3}$		$\tau(CH_2)$; def. I, III oo ph.
ν_{125}	B_1	1245	10.5	$4.3\cdot10^{-3}$		δ(CH) II, IV
ν_{124}	A	1233	123.9	$5.1\cdot10^{-2}$	1241	ν_{as}(CO); def. I, III and IIa, IVa, CT oo ph.; δ(CH) II, IV
ν_{122}	B_1	1167	4.6	$2.1\cdot10^{-3}$		ν_{as}(CO); $\omega(CH_2)$
ν_{120}	A	1158	58.4	$2.7\cdot10^{-2}$	1156	δ(CH) II, IV in ph.
ν_{113}	A	1093	20.7	$1.0\cdot10^{-2}$		$\tau(CH_3, CH_2)$; def. I, III, IIa, IVa, CT; ν(CO)
ν_{111}	A	1078	83.0	$4.2\cdot10^{-2}$	1082	Def. II, IV, CT, fur.; ν(CO)
ν_{110}	A	1060	77.8	$4.1\cdot10^{-2}$	1062	$\tau(CH_3, CH_2)$
ν_{107}	B_1	1051	13.3	$7.1\cdot10^{-3}$		$\tau(CH_3)$; $\omega(CH_2)$
ν_{105}	A	1034	23.6	$1.3\cdot10^{-2}$		δ(CH) II, IV in ph.; def of rings I–IV, CT.; $\tau(CH_2)$
ν_{102}	A	1015	106.2	$6.0\cdot10^{-2}$	1015	Def. IIb, IVb in ph.; ν(CO)
ν_{100}	B_3	985	5.6	$3.3\cdot10^{-3}$	985	$\nu(CH_2–CH_3)$ I, III oo ph.
ν_{99}	B_1	967	14.2	$8.6\cdot10^{-3}$		"Breathing" fur. oo ph.; $\nu(CH_2–CH_3)$, in-plane def of rings II, IV, CT
ν_{98}	B_2	963	11.1	$6.8\cdot10^{-3}$		"Breathing" II, IV, fur.; in-plane as def. CT
ν_{97}	A	960	250.3	0.2	936	"Breathing" IIb, IVb and CT oo ph., sym def. I, III, fur.
ν_{92}	B_3	910	2.0	$1.3\cdot10^{-3}$	891	Def. I, fur. and III, fur oo ph.; in-plane as def. IIb, IVb; $\nu(CH_2–CH_3)$
ν_{91}	B_1	904	7.1	$4.8\cdot10^{-3}$	891	As def IIb, IVb, fur., CT; $\nu(CH_2–CH_3)$
ν_{90}	B_2	899	5.9	$3.9\cdot10^{-3}$	891	Def. fur.; in-plane as def. I, III; as def. CT; $\nu(CH_2–CH_3)$
ν_{89}	B_1	896	5.7	$3.8\cdot10^{-3}$	891	Def. fur.; in-plane as def. I, III; as def. CT; $\nu(CH_2–CH_3)$
ν_{88}	B_3	895	1.2	$8.3\cdot10^{-4}$	891	In-plane as def. II, IV; as def. CT.; def. I, III oo ph.; $\nu(CH_2–CH_3)$
ν_{87}	A	877	323.4	0.2	915	"Breathing" I–IV and CT oo ph.; $\delta(\angle COC)$; $\tau(CH_3)$
ν_{86}	B_2	854	6.6	$4.8\cdot10^{-3}$	857	γ_{as}(CH) II, IV in ph.
ν_{81}	A	768	23.1	$2.0\cdot10^{-2}$	774	$r(CH_2, CH_3)$; def. I, III and II, IV, CT oo ph.; $\nu(CH_2–CH_3)$
ν_{72}	A	711	9.1	$8.6\cdot10^{-3}$	710	Out-of-plane def. I, III oo ph.
ν_{67}	B_2	674	0.5	$4.8\cdot10^{-4}$		Out-of-plane def. I, III oo ph.; out-of-plane def. fur.; $\delta(\angle C_{benz}–CH_2–CH_3)$
ν_{66}	B_1	668	18.8	$2.0\cdot10^{-2}$	682	$r(CH_2)$; in-plane as def. II, IV
ν_{63}	B_3	650	13.6	$1.5\cdot10^{-2}$	632	γ(CH) II, IV oo ph.; out-of-plane def. IIa, IVa oo ph.
ν_{59}	B_3	620	0.1	$1.3\cdot10^{-4}$		Out-of-plane def. I and III in ph; out-of-plane def. II, IV oo ph.; $\delta(\angle C_{benz}–CH_2–CH_3)$
ν_{58}	A	593	15.5	$1.9\cdot10^{-2}$	598	In-plane def. IIb, IVb in ph. and CT oo ph.
ν_{56}	B_2	548	0.7	$1.0\cdot10^{-3}$		In-plane def. I, III in ph.; def. IIb, IVb oo ph.; $r(CH_3)$; $\delta(\angle C_{benz}–CH_2–CH_3)$
ν_{51}	A	509	8.8	$1.4\cdot10^{-2}$	512	In-plane rocking of fur in ph.; in-plane def. of I, III and IIa, IVa oo ph.

TABLE 2. (Continued)

Mode	Symmetry	ν, cm^{-1}	S_i, $Å^4$ /a.m.u.	I_i	R=$C_{11}H_{23}$ (exp.)	Vibration type
ν_{47}	B_2	476	0.4	$7.0 \cdot 10^{-4}$		In-plane sym def. II and IV oo ph.; $\delta(\angle C_{benz}–CH_2–CH_3)$
ν_{40}	A	397	2.9	$6.4 \cdot 10^{-3}$	374	Out-of-plane def. I–IV, fur., CT
ν_{39}	B_2	392	0.1	$2.0 \cdot 10^{-4}$		Out-of-plane def. I–IV, fur., $\delta(\angle C_{benz}–CH_2–CH_3)$
ν_{37}	A	362	15.2	$3.9 \cdot 10^{-2}$	353	Out-of-plane rocking I–IV
ν_{33}	A	308	3.4	$1.1 \cdot 10^{-2}$	342	"Breathing" I–IV, fur., CT in ph.
ν_{28}	B_3	271	2.0	$8.2 \cdot 10^{-3}$	273	Out-of-plane def. II and IV oo ph.; $\delta(\angle C_{benz}–CH_2–CH_3)$
ν_{27}	A	254	34.1	0.2	235	$r(CH_3)$; "breathing" of microcycle in ph.
ν_{21}	A	211	15.4	$9.2 \cdot 10^{-2}$	220	"Breathing" I, III, CT and II, IV oo ph.; $\tau(CH_3)$
ν_{20}	B_3	209	4.1	$2.5 \cdot 10^{-2}$	192	Out-of-plane def. I–IV, fur., CT
ν_{19}	B_2	198	3.2	$2.0 \cdot 10^{-2}$	192	Out-of-plane def. I–IV, CT
ν_{16}	A	164	0.6	$5.2 \cdot 10^{-3}$	165	Out-of-plane def. I–IV and fur.
ν_{15}	B_1	141	2.4	$2.9 \cdot 10^{-2}$	142	$r(CH_3, CH_2)$; in-plane rocking of rings IIb and IVb oo ph
ν_{12}	B_2	125	59.0	$8.6 \cdot 10^{-2}$	115	Out-of-plane rocking IIb, IVb in ph.
ν_{11}	A	93	0.4	$1.1 \cdot 10^{-2}$		Out-of-plane whole skeleton rocking oo ph
ν_{10}	B_3	87	5.3	0.2	84	Out-of-plane rocking IIb, IVb oo ph.
ν_9	B_2	72	2.1	$8.7 \cdot 10^{-2}$		$r(CH_3, CH_2)$; out-of-plane skeleton rocking
ν_8	B_3	72	1.1	$4.4 \cdot 10^{-2}$		$r(CH_3, CH_2)$; out-of-plane skeleton rocking
ν_2	B_1	34	0.01	$1.6 \cdot 10^{-3}$		Out-of-plane whole skeleton rocking in ph
ν_1	B_1	33	0.02	$3.0 \cdot 10^{-3}$		Out-of-plane whole skeleton rocking in ph

Note. Abbreviations are the same as in Table 1; $b(CH_2)$, methylene scissors vibration; $\omega(CH_2)$, wagging vibration; $r(CH_2)$ and $r(CH_3)$, swinging vibrations; $\tau(CH_2)$ and $\tau(CH_3)$, twisting vibrations.

A line at 1443 cm^{-1} in the experimental Raman spectrum of undecane solution [17] belonged to asymmetric bending vibrations of methyls and scissors vibrations of methylenes (ν_{calc} = 1474 cm^{-1}). A line at 1305 cm^{-1} (ν_{calc} = 1299 cm^{-1}) belonged to twisting and wagging vibrations of methylenes. A line at 1137 cm^{-1} (ν_{calc} = 1125 cm^{-1}) corresponded to $\tau(CH_2)$ vibrations mixed with $\tau(CH_3)$ in addition to symmetric skeleton vibrations ν(CCCC). Thus, replacing undecyl substituents by ethyls for calculation of the Raman spectrum gave adequate positions for lines corresponding to alkyl substituent vibrations.

As a rule, swinging vibrations of methylenes were mixed with the swinging vibrations of methyls that were described above. Furthermore, swinging vibrations of methylenes were mixed with asymmetric bendings of naphthalene fragments and formed a weak line at 668 cm^{-1} (ν_{exp} = 682 cm^{-1}).

Ring vibrations. *CC stretching vibrations ν(CC) in benzene and naphthalene fragments.* Lines corresponding to CC stretching vibrations in aromatic compounds are usually observed in experimental Raman spectra in the range 1625–1430 cm^{-1} [16]. The calculations gave frequency 1603 cm^{-1} for ν(CC) vibrations of symmetry E_{2g} in the Raman spectrum of benzene; 1636 and 1460 cm^{-1} (symmetry B_{3g}) and 1580, 1463, and 1373 cm^{-1} (symmetry A_g), in the Raman spectrum of naphthalene. We calculated ν(CC) vibrations in the spectrum of *p*-2B2N of symmetry A_g and B_{3g} in the range 1637–1276 cm^{-1} (Table 1). These formed series of strong (1637, 1475, 1422, 1276 cm^{-1}) and weak (1600, 1583, 1540, 1358 cm^{-1}) lines. The line at 1637 cm^{-1} was formed by superposition of NM ν_{126} (ν_{calc} = 1637 cm^{-1}) and ν_{124} (ν_{calc} = 1628 cm^{-1}). As a rule, modes of CC benzene and naphthalene stretching vibrations that were active in the Raman spectrum were mixed (Fig. 4b). The line of ν_{107} of A_g symmetry at 1422 cm^{-1} that belonged to asymmetric vibrations of CC bonds in aromatic rings had a large amplitude (Kekule vibration) and was the strongest line in the Raman spectrum of *p*-2B2N (Table 1).

Replacing H atoms of benzene rings by ethyls caused the amplitudes of ν(CC) vibrations of benzene fragments to decrease and amplitudes of ν(CC) and bending vibrations of naphthalene fragments to increase. Vibrations ν(CC) in the Raman spectrum of *p*-2B2N4R (R = C_2H_5) in general had frequencies close to those in the spectrum of unsubstituted circulene *p*-2B2N. A frequency shift (11 cm^{-1}) upon replacing H atoms in benzene rings by ethyls occurred for the line of the most active vibration ν_{107} with frequency 1422 cm^{-1}. However, the corresponding shift in the experimental spectrum was less, only 4 cm^{-1} (ν_{exp} = 1418 cm^{-1}). A shoulder at 1446 cm^{-1} on this experimental line corresponded to a weak line of ν_{155} in the Raman spectrum of *p*-2B2N4R (R = C_2H_5) (ν_{calc} = 1446 cm^{-1}). This line contributed to ν(CC) of benzene rings and bendings of naphthalene rings (Table 2). The corresponding line ν_{111} in the spectrum of *p*-2B2N was not observed because it was too weak.

The greatest changes in the experimental spectrum of *p*-2B2N4R (R = $C_{11}H_{23}$) compared with that calculated for *p*-2B2N4R (R = C_2H_5) occurred for benzene ν(CC) vibrations with the highest frequencies to which C^2–C^3, $C^{2(3)}$–C^{α}, C10–C^{α}, and $C^{10(11)}$–C^{α} contributed. These were especially sensitive to introduction of aliphatic substituents. Thus, the line at 1637 cm^{-1} that was formed by superposition of lines at 1637 and 1628 cm^{-1} did not shift upon replacing H atoms of benzene rings by ethyls. However, two lines at 1661 and 1637 cm^{-1} in the experimental spectrum of *p*-2B2N4R (R = $C_{11}H_{23}$) corresponded to them. In our opinion, such a significant frequency shift was related to a deviation of the geometric parameters of *p*-2B2N4R (R = $C_{11}H_{23}$) from those calculated as a result of intermolecular interactions of the long aliphatic substituents upon forming the solid phase. These acted as long antennae to transfer the effect of intermolecular interactions in the condensed phase onto the geometric parameters of C–C bonds and; therefore, onto the frequencies of their vibrations.

Lines at 1603 and 1581 cm^{-1} in the spectrum of *p*-2B2N4R (R = C_2H_5) corresponded to a broad line in the spectrum of *p*-2B2N with maxima at 1600 and 1583 cm^{-1}. However, the first of these, which was due to modes of symmetry A_{2g} of frequency 1592 cm^{-1} that were forbidden in Raman spectra of 4B and 4N, was overlapped by a stronger line at 1638 cm^{-1}. It was observed in the experimental spectrum as a separate line of medium intensity at 1613 cm^{-1}.

Stretching vibrations of CC and CO in furan rings. The vibration of the $C^{\beta}C^{\beta'}$bond of symmetry A_1 in free furan (point group C_{2v}) was active in IR and Raman spectra and had frequency 1380 cm^{-1} [17] (ν_{calc} = 1387 cm^{-1}). This vibration in Raman spectra of *p*-2B2N and *p*-2B2N4R (R = C_2H_5) was split and mixed with other types of vibrations in the range 1637–1335 cm^{-1}. In the experimental spectrum, $\nu(C^{\beta}C^{\beta'})$ contributed to vibrations with frequencies 1661, 1542, 1486, and 1346 cm^{-1}.

Asymmetric vibrations of $C^{\alpha}C^{\beta}$ bonds of symmetry B_2 were calculated for free furan at 1565 cm^{-1}. The corresponding vibrations in the Raman spectrum of *p*-2B2N of symmetry B_{3g} had calculated frequencies 1628 and 1600 cm^{-1} that were determined by the contribution to NM of symmetric ν(CC) of naphthalene (ν_{124}) and benzene ($\nu_{12}1$) rings (ν_{exp} = 1637 and 1613 cm^{-1}).

Symmetric vibrations of $C^{\alpha}C^{\beta}$ bonds of symmetry A_1 were more active in the Raman spectrum of furan than asymmetric ones (ν_{calc} = 1483 cm^{-1}, ν_{exp} = 1485 cm^{-1} [17]). Vibrations $\nu_s(C^{\alpha}C^{\beta})$ in the Raman spectrum of *p*-2B2N had calculated frequency 1475 cm^{-1} (NM ν_{114} of symmetry A_g). Skeletal vibrations of aromatic C–C bonds made the main contribution to the NM. A line at 1486 cm^{-1} in the experimental spectrum of *p*-2B2N4R (R = $C_{11}H_{23}$) corresponded to these vibrations.

We calculated vibrations of CO bonds in free furan at 1065 and 992 cm^{-1} [ν_s(CO)] and 1184 and 1040 cm^{-1} [ν_{as}(CO)]. These vibrations were split in the Raman spectrum of *p*-2B2N and were mixed with δ(CH), in-plane deformations of rings, and other types of vibrations in the range 1381-1046 cm^{-1} (Table 1). Ring bending resulted in several NM (ν_{82}, ν_{91}) of ν(CO) vibrations occurring only in the furan half-ring.

The frequencies of NM contributing to ν(CO) underwent a significant shift upon introducing ethyl substituents (Tables 1 and 2). In our opinion, this was related to an increased C^{α}–O bond length after adding the ethyl substituents. Mode ν_{91} [in the Raman spectrum of *p*-2B2N4R (R = C_2H_5), it corresponded to mode ν_{122}] gave the greatest frequency shift (41 cm^{-1} to lower frequencies). However, this mode and most other NM that contributed to ν(CO) did not give detectable lines in the Raman spectrum because of their weakness. In the experimental spectrum of *p*-2B2N4R (R = $C_{11}H_{23}$), ν(CO) contributed to vibrations with frequencies 1290 and 1241 cm^{-1} (shoulder).

Bending vibrations of rings. In-plane skeletal bending of benzene, naphthalene, and furan rings and CT were observed as breathing and ring distension (Tables 1 and 2). Many of them were mixed with other types of vibrations.

In-plane skeletal bendings in the Raman spectrum of *p*-2B2N were calculated below 1452 cm^{-1}. These vibrations in the range 1452–985 cm^{-1} were mixed with δ(CH) and ν(CO) (Table 1). Breathing of rings was present in modes ν_{73} (ν_{calc} = 985 cm^{-1}), ν_{35} (ν_{calc} = 543 cm^{-1}), and ν_{21} (ν_{calc} = 372 cm^{-1}). All these modes had symmetry A_g. Lines at 960 cm^{-1} (ν_{exp} = 936 cm^{-1}), 545 and 308 cm^{-1} (ν_{exp} = 342 cm^{-1}), and 211 cm^{-1} (ν_{exp} = 220 cm^{-1}) corresponded to them in the spectrum of substituted *p*-2B2N4R (R = C_2H_5). The line at 545 cm^{-1} was very weak (I_{rel} = $5.3 \cdot 10^{-4}$). Therefore, it was not observed in the Raman spectrum. Breathing of rings in calculated Raman spectra of benzene and naphthalene gave strong lines at 988 cm^{-1} (symmetry A_{1g}) and 752 cm^{-1} (symmetry A_g); in the spectrum of furan, a strong line at 1139 cm^{-1} and a line of medium intensity at 1065 cm^{-1} of symmetry A_1. The results showed that breathing vibrational modes experienced a frequency shift upon forming *p*-2B2N and upon introducing alkyl substituents.

In-plane bendings were observed as bendings of separate fragments and as rocking of the skeleton of the whole molecule. Weak lines in the Raman spectrum of *p*-2B2N4R (R = C_2H_5) at 711, 650, 397, 362, 271, 209, 198, 164, 125, and 87 cm^{-1} belonged to out-of-plane ring bendings; at 668, 593, and 509 cm^{-1}, to in-plane ring bendings. Lines of out-of-plane bendings at 710, 632, 374, 353, 273, 192, 165, 115, and 84 cm^{-1} and in-plane bendings at 682, 598, and 512 cm^{-1} in the experimental spectrum corresponded to them (Table 2). Only several of them are shown in Fig. 3 because of the weak intensity.

Vibrations of CC bonds in alkyl substituents. Skeletal vibrations of C–C bonds of ethyl substituents (CH_2–CH_3 vibrations) appeared in the range 1008–895 cm^{-1}. These vibrations were mixed with skeletal ring bendings and gave weak lines at 985 cm^{-1} (ν_{100}) and 904 cm^{-1} (ν_{92}-ν_{88}) in the spectrum of *p*-2B2N4R (R = C_2H_5). The weak lines calculated above corresponded to very weak lines at 985 and 891 cm^{-1} in the experimental Raman spectrum of *p*-2B2N4R (Table 2). Bending of C_{benz}–CH_2–CH_3 angles was calculated by us in the range 706–271 cm^{-1}. However, the activity of the corresponding NM was very weak (<2 $Å^4$/a.m.u.). The contribution of bending of C_{benz}–CH_2–CH_3 angles could contribute in the experimental spectrum of *p*-2B2N4R (R = $C_{11}H_{23}$) to the weak line at 273 cm^{-1} (ν_{calc} = 271 cm^{-1}).

The stretching vibration of the C_{benz}–CH_2 bond occurred at greater frequency than the vibration of the CH_2–CH_3 bond and contributed to NM ν_{123}, which belonged to symmetric CO stretching vibrations of furan rings (ν_{calc} = 1223 cm^{-1}).

Conclusion. The experimental Raman spectrum of tetraoxa[8]circulene derivative *p*-dinaphthaleno-2,3,10,11-tetraundecyldiphenylenofuran was interpreted based on density functional theory (DFT) calculations. Equilibrium molecular structures, frequencies of harmonic vibrations, and activities of vibrational modes in Raman spectra were calculated using the DFT/B3LYP method in basis 6-31G(d) for unsubstituted *p*-dinaphthalenodiphenylenotetrafuran (*p*-2B2N) and *p*-dinaphthaleno-2,3,10,11-tetraethyldiphenylenotetrafuran (*p*-2B2N4R, R = C_2H_5). The calculated activities of NM were transformed into intensities. All 138 NM of *p*-2B2N and 210 NM of *p*-2B2N4R (R = C_2H_5) were calculated and analyzed. Vibrations of the studied tetraoxa[8]circulenes were compared with the calculated NM of benzene, naphthalene, furan, tetraphenylenotetrafuran and tetranaphthalenotetrafuran in order to classify the vibrations of the studied tetraoxa[8]circulenes. Several forbidden vibrational modes of these compounds became active in Raman spectra of unsubstituted and substituted tetraoxa[8]circulene *p*-2B2N4R. Correlation diagrams of NM of the studied molecules and their close structural analogs that considered the symmetry were very useful for analyzing the vibrational frequencies. A comparison of the calculated vibrational spectra and the experimental Raman spectra enabled the observed lines in the Raman spectrum of *p*-2B2N4R (R = $C_{11}H_{23}$) to be assigned. An explanation was given for the corresponding frequency shifts. The calculated spectra also helped to assign closely spaced lines for vibrations of various fragments that were superimposed in the experimental spectrum.

Those NM that corresponded to vibrations of bonds that were sensitive to aliphatic substituents underwent significant frequency shifts upon introducing substituents. The calculated frequencies of stretching and bending vibrations in the Raman spectrum of substituted *p*-2B2N4R agreed well with the experimental values. Deviations could be related to crystal packing effects. Calculations by the DFT method made it possible to explain features of the experimental spectrum of *p*-2B2N4R (R = *n*-$C_{11}H_{23}$).

REFERENCES

1. H. Erdtman and H. E. Hogberg, *Chem. Commun*., 773–774 (1968).
2. K. Yu. Chernichenko, V. V. Sumerin, R. V. Shpanchenko, E. S. Balenkova, and V. G. Nenajdenko, *Angew. Chem., Int. Ed*., **45**, No. 44, 7367–7370 (2006).
3. K. Yu. Chernichenko, E. S. Balenkova, and V. G. Nenajdenko, *Mendeleev Commun*., **18**, No. 4, 171–179 (2008).
4. C. B. Nielsen, T. Brock-Nannestad, T. K. Reenberg, P. Hammershoj, J. B. Christensen, J. W. Stouwdam, and M. Pittelkow, *Chem. Eur. J*., **16**, No. 44, 13030–13034 (2010).
5. J. Eskildsen, T. Reenberg, and J. B. Christensen, *Eur. J. Org. Chem*., **2000**, No. 8, 1637–1640 (2000).
6. T. Brock-Nannestad, C. B. Nielsen, M. Schau-Magnussen, P. Hammershoj, T. K. Reenberg, A. B. Petersen, D. Trpcevski, and M. Pittelkow, *Eur. J. Org. Chem*., No. 31, 6320–6325 (2011).
7. A. Dadvand, F. Cicoira, K. Yu. Chernichenko, E. S. Balenkova, R. M. Osuna, F. Rosei, V. G. Nenajdenko, and D. F. Perepichka, *Chem. Commun*., No. 42, 5354–5356 (2008).
8. B. F. Minaev, G. V. Baryshnikov, and V. A. Minaeva, *Comput. Theor. Chem*., **972**, No. 1–3, 68–74 (2011).
9. V. A. Minaeva, B. F. Minaev, G. V. Baryshnikov, H. Agren, and M. Pittelkow, *Vib. Spetrosc*., **61**, 156–166 (2012).
10. B. O. Minaeva, B. P. Minaev, G. V. Barynishkov, O. M. Romeiko, and M. Pittelkow, *Visn. Cherkas. Univ., Ser. Khim. Nauk*, **227**, No. 14, 39–59 (2012).
11. M. J. Frisch, G. Trucks, H. Schlegel, G. Scuseria, M. Robb, J. Cheeseman, J. Montgomery, J. Vreven, K. Kudin, J. Burant, J. Millam, S. Iyengar, J. Tomasi, V. Barone, B. Mennucci, M. Cossi, G. Scalmani, N. Rega, G. Petersson, H. Nakatsuji, M. Hada, M. Ehara, K. Toyota, R. Fukuda, J. Hasegawa, M. Ishida, T. Nakajima, Y. Honda, O. Kitao, H. Nakai, M. Klene, X. Li, R. J. Knox, H. Hratchian, J. Cross, V. Bakken, C. Adamo, J. Jaramillo, R. Gomperts, R. Stratmann, O. Yazyev, A. Austin, R. Cammi, C. Pomelli, J. Ochterski, P. Ayala, K. Morokuma, G. Voth, P. Salvador, J. Dannenberg, V. Zakrzewski, S. Dapprich, A. Daniels, M. Strain, O. Farkas, D. Malick, A. Rabuck, K. Raghavachari, J. Foresman, J. Ortiz, Q. Cui, A. Baboul, S. Clifford, J. Cioslowski, B. Stefanov, G. Liu, A. Liashenko, P. Piskorz, I. Komaromi, R. Martin, D. Fox, T. Keith, M. Al-Laham, C. Peng, A. Nanayakkara, M. Challacombe, P. Gill, B. Johnson, W. Chen, M. Wong, C. Gonzalez, and J. Pople, *Gaussian 03*, Revision C.02, Gaussian Inc., Wallingford CT (2004).
12. A. P. Scott, *J. Phys. Chem*., **100**, No. 41, 16502–16513 (1996).
13. P. L. Polavarapu, *J. Phys. Chem*., **94**, 8106–8112 (1990).
14. G. Keresztury, S. Holly, G. Besenyei, J. Varga, A. Wang, and J. R. Durig, *Spectrochim. Acta*, **49**, 2007–2026 (1993).
15. S. I. Gorelsky, SWizard Program, University of Ottawa, Ottawa, Canada (2010); http://www.sg-chem.net/
16. G. Socrates, *Infrared and Raman Characteristic Group Frequencies — Tables and Charts*, 3rd Ed., J. Wiley & Sons, Chichester (2001), pp. 54, 158–160.
17. The official web site of the National Institute of Advanced Industrial Science and Technology (AIST), Research Information Database (RIO-DB); http://riodb.ibase.aist.go.jp/riohomee.html